INSTITUTE OF PLASMA PHYSICS

NAGOYA UNIVERSITY

Single-Electron Capture into Ar^{+} Excited States in Ar^{2} + Na Collision below 12 keV.

I. Absolute Measurement of Emission Cross-Section.

Atsushi MATSUMOTO,[†] Seiji TSURUBUCHI,[†]
Kazuhiko OKUNO,[††] Shunsuke OHTANI,
Tsuruji IWAI and Yozaburo KANEKO

IPPJ-410 Aug. 1979

RESEARCH REPORT

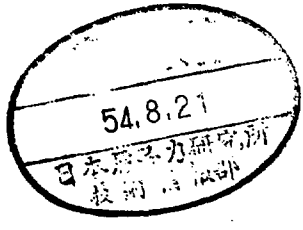

NAGOYA, JAPAN

Single-Electron Capture into Ar^{+} Excited States in Ar^{2} + Na Collision below 12 keV.

I. Absolute Measurement of Emission Cross-Section.

Atsushi MATSUMOTO,† Seiji TSURUBUCHI,†
Kazuhiko OKUNO,†† Shunsuke OHTANI,
Tsuruji IWAI and Yozaburo KANEKO

IPPJ-410 Aug. 1979

(Received July 24 1979)

Further communication about this report is to be sent to the Research Information Center, Institute of Plasma Physics, Nagoya University, Nagoya, Japan.

---

† Permanent address: Department of Physics, Faculty of Science, Osaka University, Toyonaka, Osaka 560.

†† Permanent address: Department of Physics, Faculty of Science, Tokyo Metropolitan University, Setagaya-ku, Tokyo 158.

Abstract

Emission spectra between 2800 and 6000 A have been observed at the ionic energies from 0.2 to 12 keV. Absolute measurements of emission cross-sections have been made for the emission lines coming from ArII excited states at 4 and 8 keV with a crossed-beam technique. Processes of single-electron capture into the ArII 4p- and 4p'-states, with exothermicity of a few eV, take place dominantly ($\sim 10^{-15}$ cm^2), while the endothermic processes producing ArII in the 4d- and 5s-states occur with small cross-sections. Sum of the cross-sections for electron capture into the excited states observed is comparable with the total single-electron capture cross-section estimated from attenuation measurements of ion currents. Possible errors and uncertainties are discussed.

§1. Introduction

The study of electron capture by multiply charged ions (MCI) in atoms and molecules has extensively been made in a low or intermediate energy region during the last few years.

Experimental work was done early by Hasted and his colleagues for single-electron capture by N^{2+}, Ar^{2+} and $Kr^{2,3+}$ in rare gas atoms.[1,2] Zwally and Koopman studied electron capture by C^{4+} in rare gas atoms below 40 keV in 1970.[3] Since then experimental activity in this field has grown up rapidly and the collision process involving MCI has been attacked at a number of laboratories. Salzborn's group in Giessen carried out systematic investigations on capture of one or more electrons by MCI of rare gas in atoms below 100 keV.[4-7] Gilbody's group in Belfast examined electron capture by Li^{3+} in H and H_2 at the energies 65 to 1500 keV.[8] Phaneuf, Meyer and McKnight at ORNL reported electron capture by MCI of N, O and C in H and H_2 at the energies 10 to 1650 keV.[9] Okuno, Koizumi and Kaneko, quite recently, have studied symmetric resonant double charge transfer for the system of Kr^{2+} + Kr and Xe^{2+} + Xe at the low energy below 20 eV.[10] Theoretical work has actively been done in connection with the needs from fusion plasmas, so that almost all the theories deal with collisions between fully-stripped ions and atomic hydrogen.[11-15]

When a projectile ion A^{q+} (q>1) collides with a target atom B, multiple-electron capture processes can take place, but the dominant process is usually single-electron capture,

$$A^{q+} + B \rightarrow A^{(q-1)+*} + B^{+} + \Delta E. \qquad (1.1)$$

Here ΔE stands for the change in the total internal energy of the initial and final states at infinite internuclear separations. In this reaction, there are many possible channels connecting with excited states of projectile as well as its ground state. For electron capture by MCI into the ground state, ΔE is so large that a very small cross-section is predicted according to the Massey criterion. On the other hand, a capture process into some excited state has a small energy defect; it will be dominant at low or intermediate energies. This prediction leads to the possibility of soft X-ray lasers[16,17] and relates closely to a serious problem in fusion plasmas, i.e., plasma cooling by radiation of emission lines from MCI.[18]

In spite of such a circumstance, most of the experimental studies have been restricted to determination of the cross-section of total electron capture. There has been little work on electron capture into excited states. The group of FOM Institute has taken the initiative in this area. Winter, Bloemen and de Heer have optically determined the cross-sections for electron capture into excited states of projectile in the collisions of Ne^{q+} (q=1,2,3,4) with He at the energies 25 to 800 keV[19] and with He, Ar and H_2 at 100 keV.[20]

Aiming at application to atomic collision experiments, we have constructed a multiply-charged-ion source, where MCI is produced by bombardments of hot electrons in the so-called ECR-

plasmas.[21] As a first trial, we have studied single-electron capture into the ArII excited states in the collisions of Ar^{2+} with Na by means of absolute measurements of light emission intensities with a crossed-beam technique at the ionic energies below 12 keV. For the present collision system, there are a large number of channels opened to excited states of projectile. Such a complicated system, in turn, should contain much information on production rates of individual excited states. This is one of the reasons why the present system was chosen. A second reason is that the present study can be a model experiment for electron capture by MCI in atomic hydrogen, because Na has one s= electron in the outer-shell and neither excitation nor ionization of Na^{+} are expected owing to its large endothermicity. Other reasons come from experimental facilities; a stable and intense ion beam of Ar^{2+} can be obtained easily, and no differential pumping system is necessary, because sodium atoms are effectively trapped.

§ 2. Experimental

2a) Experimental setup

It is necessary to produce an intense and stable ion beam in the desired charge state for the study of collision processes involving multiply charged ions. For the purpose, we have constructed one of the new devices for producing highly charged ions, an ECR ion source, which is based on electron-cyclotron-resonance (ECR) heating of plasmas in a magnetic bottle. Its detailed description is found in ref. 21.

The experimental setup is sketched in Fig. 1. An ion beam extracted from the ion source was mass-analysed, and then was led through a collimating slit (1.1mm-wide, 2.3mm-high) into a collision chamber. The ion beam was crossed at right angles with an effusing beam of sodium atoms and was received with a Faraday cup after running a few cm in the collision chamber. Typical ion currents were a few μA for Ar^+ and Ar^{2+}. Radiation from the crossing region was observed along the third orthogonal direction through a sapphire window. The light flux was focused with a quartz condensing lens on the entrance slit of a quartz spectrograph (Hilger D96, f/1.8) or of a grating monochromator (Nikon G250, f/4.5). A photomultiplier (HTV R376) with a d.c. amplifier was used for photoelectric measurements.

The beam of sodium atoms was produced by effusion from an orifice (1.1mm-diameter, 1.5mm-thick) which was drilled on a removable cap of an oven. The orifice was placed at 9.3 mm distance from the center of the ion beam. The oven was made

of stainless steel and its temperature was monitored with an alumel-chromel thermocouple attached to the oven. A plate shutter was placed in front of the orifice to stop the atomic beam for background measurements and during warming-up periods. A liquid nitrogen trap was placed above the crossing of both the beams, and sodium atoms were effectively condensed on the trap after running several cm.

The collision chamber was evacuated with a 4-inch oil-diffusion pump together with a cold trap. The back pressure was maintained below 1×10^{-6} Torr. The transparency of radiation through the sapphire window suffers from a very small amount of contamination of sodium. Therefore, the window was heated to prevent it from any contamination throughout measurements of light intensities.

2b) Experimental procedure

If it is assumed that radiation emerging from the crossing is isotropic, the cross-section Q_λ for the emission of photons at wavelength λ is given by

$$Q_\lambda = \frac{4\pi}{\omega} \frac{q\,e}{I_i\, N\, L} \frac{S_\lambda}{h\nu} k(\lambda)^{-1}, \qquad (2.1)$$

where qe is the charge of a projectile ion, I_i the ion beam current, ω the solid angle subtended by the condensing lens at the crossing, L the observation length along the axis of the ion beam, N the target atom density at the observed region, $h\nu$ the energy of emitted photons, S_λ the photomultiplier signal current, and $k(\lambda)$ overall

sensitivity of the optical detection system. The quantities ω and L follow from the geometry of the optical arrangement. Then, if the target density and the sensitivity are determined, we can evaluate the emission cross-section.

The target density N is derived from the relation, $N = I_a/\langle v \rangle$, where I_a and $\langle v \rangle$ are the beam intensity and the mean velocity of target atoms, respectively. Two conventional techniques may be available to determine the beam intensity of sodium atoms; surface ionization and deposition.[22] The latter one was adopted in the present work. The sodium atomic beam was condensed, after passing through the ion beam, on a circular stainless-steel plate (17mm= radius) attached at the bottom of the liquid nitrogen trap. The distance between the plate and the orifice was set at 102 mm. After each experimental run of some ten hours, the plate was removed and sodium layer deposited on it was dissolved into a known amount of water. Sodium concentration of the solution was compared with that of a standard solution of NaOH by the method of atomic absorption.[23] The beam intensity follows from the total amount of sodium atoms collected during the experimental run. The mean velocity $\langle v \rangle$ is derived from the monitored temperature, provided that the velocity distribution is Maxwellian. The target density has to be chosen sufficiently low so that secondary collision effects are negligibly small. We confirmed a good linear-relation between S_λ/I_i and N, as far as the target density ranged from 0.6 to 2.1×10^{-12} cm^{-3}; all the measurements of light intensities were made in this density range.

The spectral sensitivity of the detection system $k(\lambda)$ was determined by use of a hollow cathode lamp (Westinghouse, WL22606),

which was calibrated against a tungsten ribbon lamp calibrated by NBS (GE, 30A/T24). The calibration was made by means of a double monochromator (Spex 1400) in order to diminish stray light in the monochromator as much as possible. The hollow cathode lamp was set at just the same place as the crossing, and the same optical detection system was used for intensity measurements of radiation from the lamp and the crossing.

In order to estimate the total electron-capture cross-section σ_{21}, the attenuation of the ion current was measured. If it is assumed that the attenuation of Ar^{2+} ion current is mainly due tc single-electron capture, the total cross-section σ_{21} is given by

$$\sigma_{21} = -\Pi^{-1} \ln\left(\frac{2I}{I_0} - 1\right), \qquad (2.2)$$

where Π represents a target thickness. The incident ion current I_0 attenuates to I after passing through the target beam. Both the currents I and I_0 were measured with the Faraday cup by opening and closing of the shutter placed in front of the orifice. The target thickness Π was obtained from the density distribution of the target beam along the axis of the ion beam; the distribution was estimated experimentally as follows. For the (Ar^+, Na) collision, only Na D-lines are observed, as mentioned in §3. Then, the intensity distribution of light emission reflects the density distribution of the target beam. The former was measured by means of microphotometry of the photograph of the crossing region taken through the window.

2c) Possible errors and uncertainties

The relative error in Q_λ can be estimated from eq. (2.1) as follows:

$$\left|\frac{\Delta Q_\lambda}{Q_\lambda}\right| \leq \left|\frac{\Delta I_i}{I_i}\right| + \left|\frac{\Delta N}{N}\right| + \left|\frac{\Delta S_\lambda}{S_\lambda}\right| + \left|\frac{\Delta k(\lambda)}{k(\lambda)}\right| + \left|\frac{\Delta L}{L}\right| + \left|\frac{\Delta \omega}{\omega}\right|. \qquad (2.3)$$

As for I_i, an error comes from its instability and attenuation in passing through the target beam. The instability is within ±1 % and the attenuation is smaller than 1 % under the condition of light intensity measurements. The instability in S_λ is less than ±2 %, except for the case of weak emission lines. As for $k(\lambda)$, the error arises from several components; the uncertainty in spectral radiance of the standard lamp is estimated to be ±8 %,[24] the reproducibility and instability of the hollow cathode lamp within ±3 %, an error in measurements of geometrical quantities such as slit widths ±1.5 %, and an error in measurements of photoelectric current of the standard lamp ±0.5 %; total limit of the error for $k(\lambda)$ is therefore ±13 %. As for L, an error is estimated at about ±5 %. A negligible error comes from ω, because of the same optical arrangement.

As for the derivation of target density, there are possible errors arising from five origins at least. One comes from the procedure of atomic absorption. A main error arises from preparation of the standard solution and is estimated at about ±5 %. A second error comes from the instability such as a fluctuation and drift of the oven temperature. We could not detect any instability of the monitored temperature larger than ±2.5 °C.

Even a very small instability, however, affects individual measurements through the density fluctuation seriously, because the beam density depends on the temperature exponentially. For example, the fluctuation of ±2.5°C in temperature causes the deviation of ±7 % in density for the present case. Another problem comes from the derivation of the mean velocity. We derived it from the monitored temperature, which may be different from the temperature defined in the atomic beam. A gas kinetic treatment enables us to estimate the latter temperature; the ambiguity in estimated temperature is ±4 % which corresponds to an error of ±2 % in $\langle v \rangle$, since the mean velocity is proportional to the square root of temperature. A fourth error results from measurements of geometrical dimensions. This induces an error of ±7 % in N. A fifth problem lies at the assumption that the condensation coefficient of sodium atom is unity. Wexler pointed out [25] that alkali atoms stick well to oxide-free metallic surfaces at the temparature far below 25°C. Thus we have made the above assumption, but uncertainty still remains. An inevitable error in determination of the target density is estimated to be about ±21 % for absolute measurements and about ±7 % for relative measurements.

We have so far been concerned with possible errors arising from determination of each quantity in eq. (2.1). Evaluation of emission cross-sections from eq. (2.1) is based on at least three assumptions, of which validity depends on experimental conditions. As mentioned above, an isotropic radiation was assumed. The light emission from a collision volume, however, is in general polarized and its intensity has an angular dependence. The polarization effect is usually pronounced at low-energy collisions;

a systematic error then comes into the energy dependence of emission cross-sections. The polarization effect was not examined in the present experiment and no correction was made.

A second problem relates to the lifetime effect. As far as radiation from the projectile is concerned, the light emission tails away along the direction of the ion beam. This tailing originates in a definite lifetime of the excited states from which the emission lines come. Therefore, the effect will be enhanced in an emission line from the state having a long lifetime and in an emitter having a high velocity. This lifetime effect causes another systematic error, but it can be corrected if the lifetime for each excited state and the density distribution of target atoms are given. The density distribution was estimated by means of microphotometry mentioned in 2b). Almost all the values of the lifetime were referred to Fink et al.[26] The rest were obtained from refs. 27-29.† The correction factor was evaluated for each emission line and at each ionic energy. A typical example is as follows; the emission intensity observed should be reduced to 94 % of its own for 3729 A-line ($4p\ ^4S_{3/2} \rightarrow 4s\ ^4P_{5/2}$) at 4 keV. Fink et al. estimated errors in their data to be about 30 %. This corresponds to errors of ±4 % and ±6 % in the present correction factor at 4 keV and 8 keV, respectively, at the extreme of the longest lifetime for the excited states observed. From measurements of the density distribution, an error comes into the correction factor by smaller than ±1 %. Thus the error in the correction factor for lifetime effect does not exceed ±7 %.

---

† The lifetime for ArII $4d\ ^2F_{5/2}$ was not available and was assumed to be the same as that for $4d\ ^2F_{7/2}$.

Equation (2.1) is valid if either the ion beam or the atomic beam is homogeneous. The homogeneity is the third assumption which is difficult to check. After all, a possible error in determination of emission cross-sections is estimated at about ±50 % for absolute measurements and at about ±18 % for relative measurements. Uncertainties remain in the condensation efficiency of sodium atoms, the polarization effect, and the homogeneity of the ion beam.

Suppose attenuation measurements of the ion current. Errors in determination of Π and $\ln(2I/I_0 - 1)$ are estimated to be ±24 % and ±15 %, respectively. A systematic error will come from the assumption that the attenuation is caused by single-electron capture only. In addition to that, an elastic scattering results in the attenuation. The maximum cone-angle of elastic scattering is 35° in the laboratory system, whereas the cone-angle which the aperture of the Faraday cup subtends at the crossing is about 20°. Therefore, only a large angle scattering contributes to the attenuation. This contribution is expected to be minor, although it can not be estimated because of a lack of data on the differential cross-section. Then eq. (2.2) gives the upper limit of σ_{21}.

A secondary collisional process, $Ar^{2+} + Na \rightarrow Ar^{+} + Na$ followed by $Ar^{+} + Na \rightarrow Ar + Na^{+}$, might be responsible for the attenuation. This process, however, can be neglected, because the attenuation of Ar^{+} ion currents was not observed in the (Ar^{+}, Na) collision under the condition of the same target density. Double-electron capture process may be also negligible, because its cross-section is usually much smaller than that for single-electron capture.

§3. Results and Discussion

3a) Survey spectra and emission cross-sections

Survey spectra were photographed for the collision system of (Ar^+, Na) and (Ar^{2+}, Na) in the wavelength region from 2800 to 6000 A at the ionic energy of several keV. For the (Ar^+, Na) collision, emission lines observed are only Na D-lines and no emission line due to either ArI or ArII is detected. On the other hand, several tens of emission lines are observed for the (Ar^{2+}, Na) collision, as shown in Fig. 2. The emission lines observed were identified as ArII lines or Na D-lines. These results indicate that single-electron capture into excited states of projectile,

$$Ar^{2+} + Na \rightarrow Ar^{+*} + Na^+ + \Delta E, \qquad (3.1)$$

takes place remarkably as well as direct excitation of target,

$$Ar^{2+} + Na(3s\ ^2S) \rightarrow Ar^{2+} + Na(3p\ ^2P), \qquad (3.2)$$

for the (Ar^{2+}, Na) collision, whereas direct excitation of target is a dominant inelastic collision process for the (Ar^+, Na) collision.

The ArII emission lines observed are from the excited states of such electron configurations as $3p^4(^3P)4p$, $3p^4(^1D)4p'$, $3p^4(^3P)4d$, and $3p^4(^3P)5s$, which are hereafter abbreviated to the 4p-, 4p'-, 4d- and 5s-states, respectively. Then transitions such as 4p →

4s or 3d, 4p' → 4s' or 3d, 4d → 4p, and 5s → 4p can be observed in the visible and near ultraviolet region. Strong emission lines arise from the 4p- and 4p'-states, while all the emission lines from the 4d- and 5s-states are weak. The 4p-state consists of thirteen terms including multiplets: $^2S_{1/2}$, $^4S_{3/2}$, $^2P_{1/2,3/2}$, $^2D_{3/2,5/2}$, $^4P_{1/2,3/2,5/2}$ and $^4D_{1/2,3/2,5/2,7/2}$. Emission lines from all the terms are observed and strong lines come from the multiplets of high-J values. Much the same feature is seen in emission lines from the 4p'-states; emission lines from all the possible terms, $^2P_{3/2,5/2}$, $^2D_{3/2,5/2}$, and $^2F_{5/2,7/2}$, are detected and strong lines come from the high-J multiplets. Meanwhile, emission lines from the 4d-state are in general weak and are limited to those from the terms of ^4P, ^4D, ^4F and ^2F; no emission line is detected from other possible terms of ^2P and ^2D. Only a few lines from the 5s-state are detectable and very weak.

These features apparent in survey spectra were confirmed quantitatively by photoelectric measurements. Absolute measurements of emission cross-sections were carried out at the ionic energies of 4 and 8 keV. Table 1 shows the values of emission cross-sections obtained. Since the number of the emission lines observed is over eighty, the cross-sections listed in the table are limited to some typical ones. Identification of transitions was referred to the table given by Striganov and Sventitskii.[30] If the primary ion Ar^{2+} is assumed to be in its ground state $3p^4\,^3P$, the energy defect ΔE in eq. (3.1) can be obtained from Moore's table.[31] The values for ΔE are also listed in Table 1. Reactions producing ArII in the 4p- and 4p'-states are exothermic ($\Delta E>0$), and we have the following relations; 3.3 eV > ΔE > 2.5 eV

for the excitation of the 4p-state, and 1.4 eV > ΔE > 1.0 eV for that of the 4p'-sate.† Reactions producing ArII in the 4d-state are endothermic ($\Delta E<0$), and we have $|\Delta E|<0.8$ eV for the detectable terms and $|\Delta E|>1$ eV for the nondetectable terms ^2P and ^2D. Large endothermicity may be the reason why the latter terms can not be observed. The excitation of the 5s-state is less endothermic than that of the 4d-state, but the transition probability for 5s → 4p is much smaller than that for 4d → 4p. From these facts, it turns out that exothermic reactions with the energy defect of a few eV take place remarkably compared with endothermic ones at the ionic energy of several keV.

The energy dependence of emission cross-sections was examined at the ionic energies from 0.2 to 12 keV for three emission lines (3729 A, 4072 A, 3559 A), which were selected as the representative of emission lines from the 4p-, 4p'- and 4d-states. The results obtained are shown in Figs. 3(a), (b) and (c), where the virtical bars indicate 95% confidence limits of random error. The energy dependence is quite different from each other. The emission cross-section for the transition 4p $^4S_{3/2}$ → 4s $^4P_{5/2}$(3729 A) has a broad maximum around 4.5 keV; the others have no maximum; the one for 4d $^2F_{7/2}$ → 4p $^2D_{5/2}$(3559 A)†† seems to be independent of energy. These results will be discussed in the following paper.

---

†If a metastable ion of $3p^4$ ^1D is responsible for the excitation of the 4p'-state, 3.1 eV > ΔE > 2.7 eV.

††The energy dependence was examined with large slit widths, so that 3559A-line was blended with some weak lines. The other two lines examined were well-separated.

3b) Excitation cross-sections

The next problem of interest is how much the electron-capture into excited states does take part in the total electron-capture. Excitation cross-sections were then evaluated from the emission cross-sections observed. The excitation cross-section for the electron-capture into the j-th term of the ArII nl-state $Q_j(nl)$ is given by

$$Q_j(nl) = \sum_k Q_{jk} - \sum_i Q_{ij} , \qquad (3.3)$$

where Q_{jk} is the emission cross-section for the transition from j to k, and the summation extends over all the possible final states k. The second term on the right-hand side is a correction for cascading effects. Actually, errors come from missing out some emission lines. Most of the emission lines from the excited states observed appear in the visible and near ultraviolet region, but the ones from the transitions 4d → 3p and 5s → 3p are outside of the detectable wavelength region. An alternative evaluation is available, if the transition probability of spontaneous emission A_{jk} and the lifetime τ_j are known;

$$Q_j(nl) = Q_{jk}/(\tau_j A_{jk}) - \sum_i Q_{ij} . \qquad (3.4)$$

In this case, errors arise from uncertainties in A_{jk} and τ_j. Values of the transition probability and lifetime were referred to Wiese et al.[32], Shumaker and Popenoe[33]

The $Q_j(nl)$ values obtained in both the ways were in agreement with each other within ±10 %. The result obtained at 4 keV is as follows:

$$Q(4p) = 3.11\times10^{-15}\ cm^2;\quad Q(4p') = 1.47\times10^{-15}\ cm^2;$$
$$Q(4d) = 0.37\times10^{-15}\ cm^2;\quad Q(5s) = 0.9\times10^{-17}\ cm^2.$$

Here $Q(nl)$ means the sum of $Q_j(nl)$ over all the terms of the nl= state. All the cross-sections are cascade-free. The sum of the excitation cross-sections observed is about $5.0\times10^{-15}\ cm^2$. These cross-sections can be compared with the cross-section for the total electron-capture σ_{21}. The upper limit of σ_{21} was estimated from attenuation measurements of ion currents (see eq. (2.2)); the value obtained in this way is $11\times10^{-15}\ cm^2$ at 4 keV. The estimated accuracy is about ±50 % in Q_{jk} and ±40 % in σ_{21}. Therefore, an accurate quantitative comparison is difficult, but it is concluded that the sum of the cross-sections for the electron-capture into the excited states observed is comparable with the total electron= capture cross-section at several-keV collisions.

There may exist electron-capture processes into other excited states such as the 3d-, 4s- and 4s'-states because of their exothermicities. These states, however, can not be detected in the present experiment, because all the emission lines from these states fall onto the vacuum ultraviolet region.

Acknowledgments

This work was supported in part by the Grant-in-Aid for Special Project Research No. 111011 from the Ministry of Education and was done under the Collaborating Research Program at Institute of Plasma Physics, Nagoya University.

References

1) J.B.Hasted, D.Phill and R.A.Smith: Proc. Roy. Soc. A235 (1956) 354.

2) J.B.Hasted and A.Y.J.Chang: proc. Phys. Soc. 80 (1962) 441.

3) H.J.Zwally and D.W.Koopman: Phys. Rev. A2 (1970) 1851.

4) E.Salzborn: IEEE Trans. Nucl. Sci. NS-23 (1976) 947.

5) H.Klinger, A.Müller and E.Salzborn: J. Phys. B8 (1975) 230.

6) H.Klinger, A.Müller and E.Salzborn: J. Chem. Phys. 65 (1976) 3427.

7) A.Müller and E.Salzborn: Phys. Lett. A59 (1976) 19.

8) M.B.Shah, T.V.Goffe and H.B.Gilbody: J. Phys. B11 (1978) L233.

9) R.A.Phaneuf, F.W.Meyer and R.H.McKnight: Phys. Rev. A17 (1978) 534.

10) K.Okuno, T.Koizumi and Y.Kaneko: Phys. Rev. Lett. 40 (1978) 1708.

11) A.Salop and R.E.Olson: Phys. Rev. A13 (1976) 1312.

12) C.Bottcher: J. Phys. B10 (1977) L213.

13) J.Vaaben and J.S.Briggs: J. Phys. B10 (1977) L521.

14) R.E.Olson, K.H.Berkner, W.G.Graham, R.V.Pyle, A.S.Schlachter and J.W.Stearns: Phys. Rev. Lett. 41 (1978) 163.

15) H.Ryufuku and T.Watanabe: Phys. Rev. A18 (1978) 2005.

16) A.V.Vinogradov and I.I.Sobel'man: Soviet Physics-JETP 36 (1973) 1115.

17) W.H.Louisell, M.O.Scully and W.B.McKnight: Phys. Rev. A11 (1975) 989.

18) R.W.P.McWhirter: IAEA-199, Atom. Molec. Data for Fusion, (1977) p.297.

19) H.Winter, E.Bloemen and F.J.de Heer: J. Phys. B10 (1977) L1.

20) H.Winter, E.Bloemen and F.J.de Heer: J. Phys. B10 (1977) L311.

21) A.Matsumoto, S.Aihara, S.Ohtani, K.Okuno, S.Tsurubuchi, T.Iwai and Y.Kaneko: Phys. Lett. (to be published).

22) J.B.Hasted: Physics of Atomic Collisions (Butterworth, London, 1972) 2nd ed., Chap. 3, p.273.

23) B.J.Russell, J.P.Shelton and A.Walsh: Spectrochim. Acta 8 (1957) 317.

24) R.Stair, R.G.Johnston and E.W.Halbach: J. Res. Nat.Bur. Stand. (USA) 64A (1960) 291.

25) S.Wexler: Rev. Mod. Phys. 30 (1958) 402.

26) U.Fink, S.Bashkin and W.S.Bickel: J.Q.S.R.T. 10 (1970) 1241.

27) J.A.Kernahan, C.C.Lin and E.H.Pinnington: J. Opt. Soc. Amer. 60 (1970) 898.

28) E.H.Pinnington, P.Weinberg, W.Verfuss, H.O.Lutz and R.Hippler: Phys. Lett. 65A (1978) 287.

29) A.Denis and M.Gaillard: Phys. Lett. 31A (1970) 9.

30) A.R.Striganov and N.S.Sventitskii: Tables of Spectral Lines of Neutral and Ionized Atoms, Transl. from Russian (IFI/Plenum, New York, 1968).

31) C.E.Moore: Atomic Energy Levels vol. 1 (NBS Circular 467, 1949).

32) W.L.Wiese, M.W.Smith and B.M.Miles: Atomic Transition Probabilities vol. 2 (NSRDS-NBS 22, 1969).

33) J.B.Shumaker,Jr and C.H.Popenoe: J. Opt. Soc. Amer. 59 (1969) 980.

Table 1. Emission cross-section Q_{jk} for $Ar^{2+}(3p^4)$ + Na → $Ar^{+}(3p^4nl;j)$ + Na^{+}; $Ar^{+}(3p^4nl;j)$ → $Ar^{+}(3p^4n'l';k)$ + hν.

Transition	λ (A)	Q_{jk} ($\times 10^{-16} cm^2$)		ΔE(eV)
		4 keV	8 keV	
4p → 4s				
$^4P_{5/2} \rightarrow {}^4P_{5/2}$	4806.017	1.39	2.67	3.26
$^4D_{7/2} \rightarrow {}^4P_{5/2}$	4348.063	3.35	7.29	2.99
$^4D_{5/2} \rightarrow {}^4P_{3/2}$	4426.005	2.25	4.84	2.94
$^2D_{5/2} \rightarrow {}^2P_{3/2}$	4879.860	2.82	5.67	2.81
$^2P_{3/2} \rightarrow {}^2P_{1/2}$	4764.862	1.58	3.09	2.62
$^4S_{3/2} \rightarrow {}^4P_{5/2}$	3729.310	2.89	2.71	2.52
$^2S_{1/2} \rightarrow {}^2P_{1/2}$	4579.346	1.21	2.45	2.51
4p' → 4s'				
$^2F_{5/2} \rightarrow {}^2D_{3/2}$	4589.896	2.31	3.15	1.36
$^2F_{7/2} \rightarrow {}^2D_{5/2}$	4609.560	4.57	5.51	1.34
$^2P_{3/2} \rightarrow {}^2D_{5/2}$	4277.524	1.17	1.90	1.14
$^2D_{5/2} \rightarrow {}^2D_{5/2}$	4072.006	1.44	1.82	0.99
4d → 4p				
$^4D_{7/2} \rightarrow {}^4P_{5/2}$	3491.538	0.27	0.28	-0.29
$^4F_{9/2} \rightarrow {}^4D_{7/2}$	3588.448	0.47	0.54	-0.46
$^2F_{7/2} \rightarrow {}^2D_{5/2}$	3559.508	0.75	0.88	-0.68
$^4P_{5/2} \rightarrow {}^4S_{3/2}$	3868.524	0.15	0.17	-0.69
5s → 4p				
$^4P_{5/2} \rightarrow {}^4P_{5/2}$	3765.269	0.09	0.18	-0.03

Figure Captions

Fig. 1. Experimental setup

①, mass analyser; ②, analyser slits; ③, oven; ④, thermocouple; ⑤, liquid nitrogen trap; ⑥, plate collecting sodium; ⑦, shutter; ⑧, Faraday cup; ⑨, sapphire window.

Fig. 2. Survey spectrum for collision of Ar^{2+} with Na at 8 keV: slit width, 30 μ; exposure time, 4 hours; film, Tri-X.

Fig. 3. Energy dependence of emission cross-sections for ArII lines. Vertical bars represent 95 % confidence limit of random error

(a) 3729A-line, $4p\ ^4S_{3/2} \rightarrow 4s\ ^4P_{5/2}$;

(b) 4072A-line, $4p'\ ^2D_{5/2} \rightarrow 4s'\ ^2D_{5/2}$;

(c) 3559A-line, $4d\ ^2F_{7/2} \rightarrow 4p\ ^2D_{5/2}$.

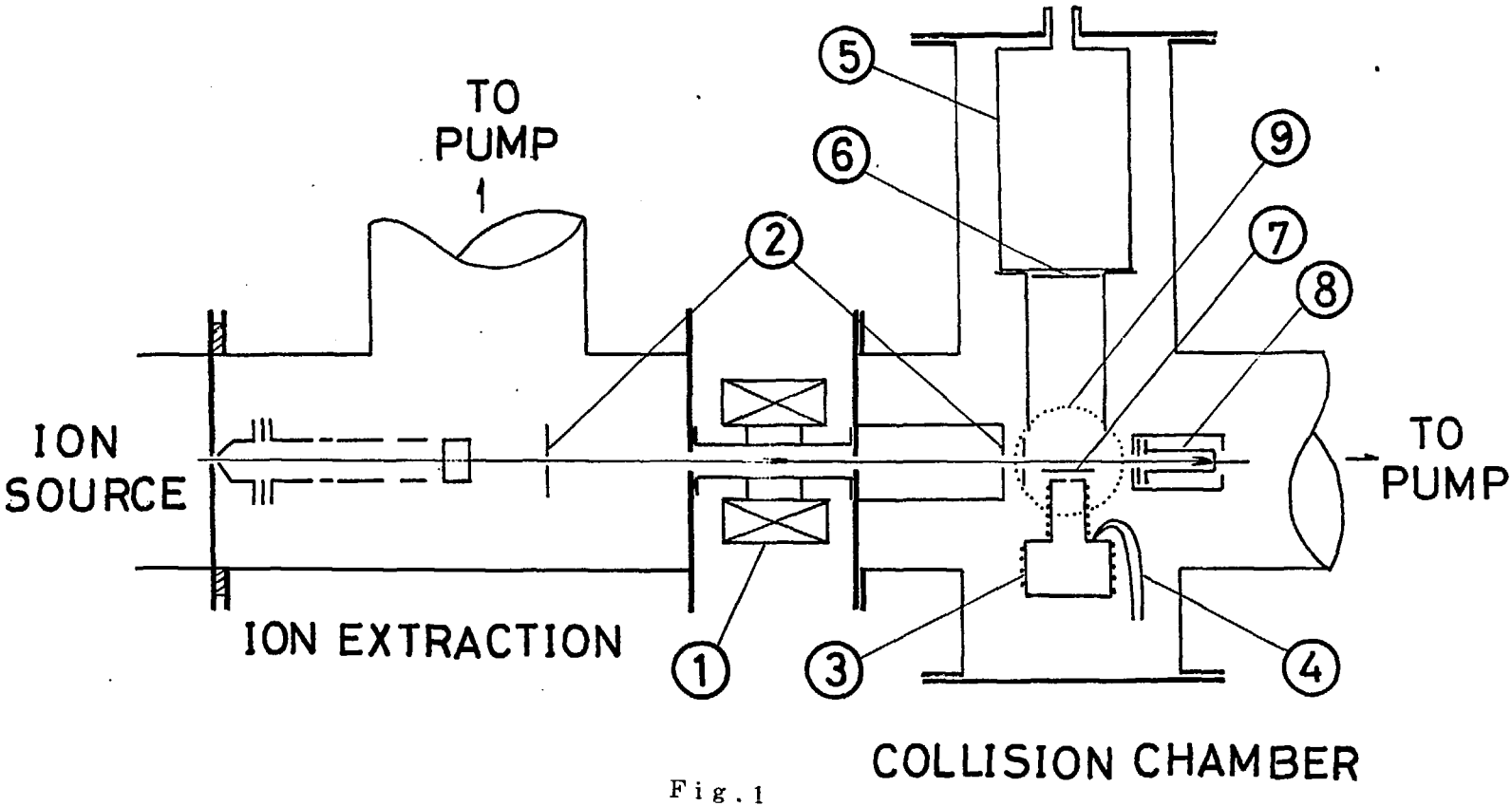
TO
PUMP
1
5
6
9
7
8
2
ION
SOURCE
TO
PUMP
ION EXTRACTION
1
3
4
COLLISION CHAMBER

Fig. 1

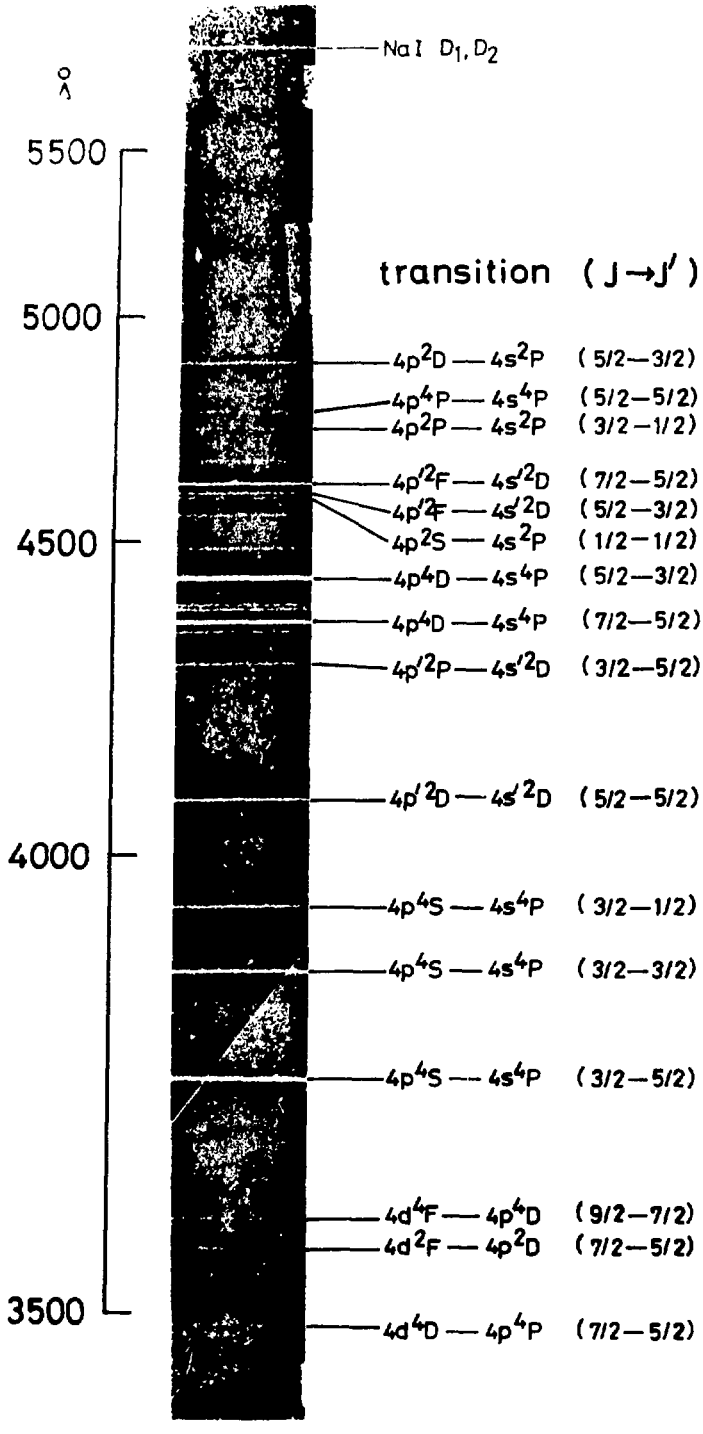
Å
5500
5000
4500
4000
3500
NaI D_1, D_2
transition (J→J')
$4p^2D - 4s^2P$ (5/2—3/2)
$4p^4P - 4s^4P$ (5/2—5/2)
$4p^2P - 4s^2P$ (3/2—1/2)
$4p'^2F - 4s'^2D$ (7/2—5/2)
$4p'^2F - 4s'^2D$ (5/2—3/2)
$4p^2S - 4s^2P$ (1/2—1/2)
$4p^4D - 4s^4P$ (5/2—3/2)
$4p^4D - 4s^4P$ (7/2—5/2)
$4p'^2P - 4s'^2D$ (3/2—5/2)
$4p'^2D - 4s'^2D$ (5/2—5/2)
$4p^4S - 4s^4P$ (3/2—1/2)
$4p^4S - 4s^4P$ (3/2—3/2)
$4p^4S - 4s^4P$ (3/2—5/2)
$4d^4F - 4p^4D$ (9/2—7/2)
$4d^2F - 4p^2D$ (7/2—5/2)
$4d^4D - 4p^4P$ (7/2—5/2)

Fig. 2

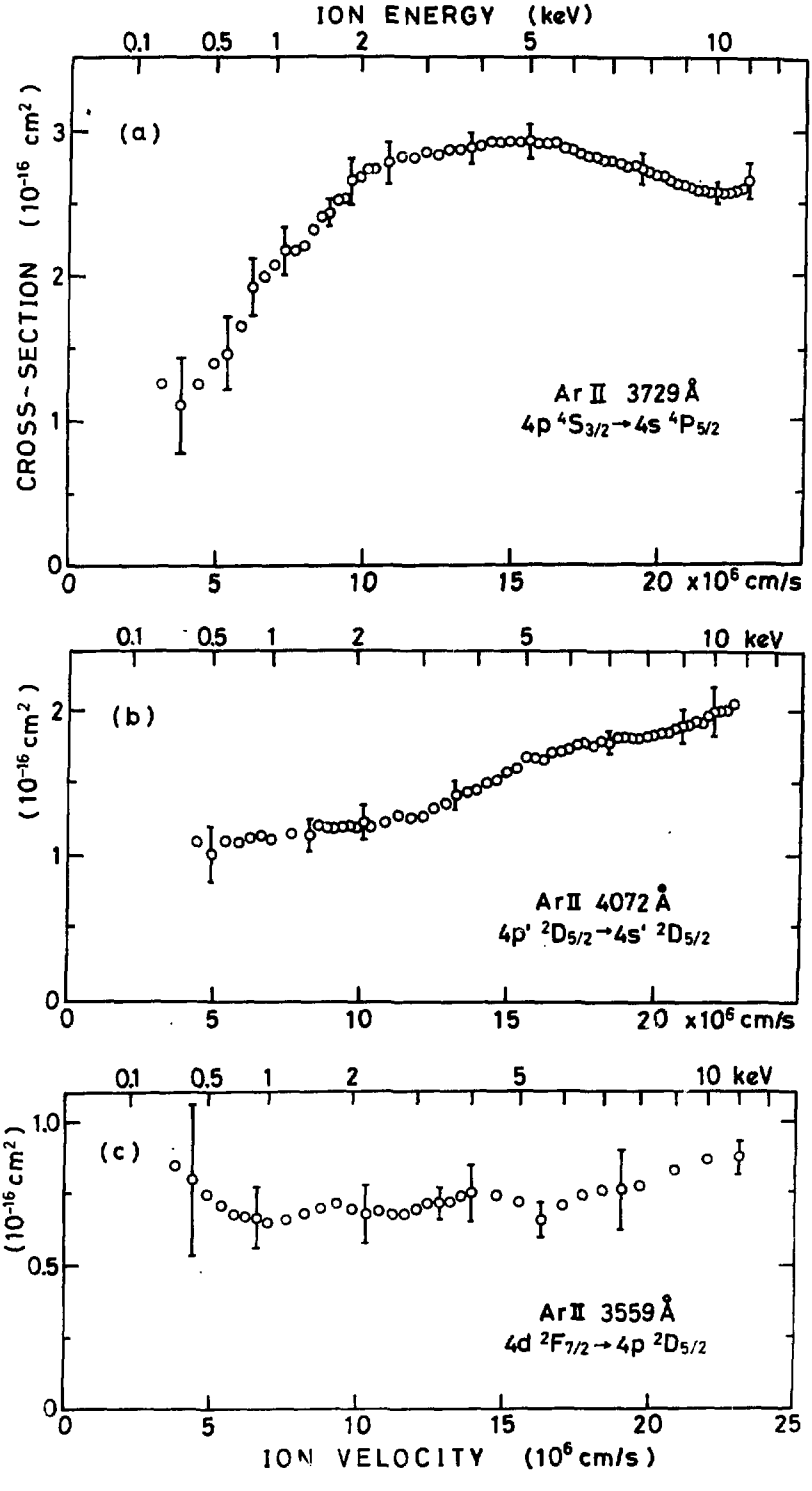
ION ENERGY (keV)
0.1
0.5
1
2
5
10
(a)
CROSS-SECTION (10⁻¹⁶ cm²)
ArII 3729 Å
4p ⁴S3/2→4s ⁴P5/2
0
5
10
15
20 x10⁶ cm/s
(b)
(10⁻¹⁶ cm²)
ArII 4072 Å
4p' ²D5/2→4s' ²D5/2
(c)
ArII 3559 Å
4d ²F7/2→4p ²D5/2
ION VELOCITY (10⁶ cm/s)

Fig. 3